

DEFORMATION AND FRACTURE – LAB COURSE

Autumn semester 2012/2013

Determination of K_{Ic}

Václav Pejchal

(based on notes by A. Miserez, augmented by C. Bacciarini,
translated from French by A. Rossoll)

1. Aim

The purpose of this lab is to determine the critical stress intensity factor, K_{Ic} , also named plane-strain fracture toughness, according to the standard AFNOR NF EN ISO 12737 (equivalent to ASTM E399). The three samples that are to be tested are made of the same steel (C45E, DIN 1.1191) but have undergone different heat treatments, such that the importance of the microstructure with regard to the fracture toughness will be put into evidence. We will also explore an alternative evaluation of fracture toughness by determining the critical value of the J -integral.

2. General

The fracture toughness, which can be determined by testing, characterizes (in a neutral environment) the **resistance** of a material that is in plane strain conditions (which is the most severe stress state) **against unstable crack propagation**. The fracture toughness corresponds to the critical value of the stress intensity factor. It can be used to determine the **relation between the strength and the size of a flaw for a material that is in service** under severe loading conditions as will be detailed below. This test is not of the usual kind in the sense that it cannot be assured beforehand that a valid test result will be obtained. This is why it is absolutely necessary that all validity criteria be verified in all rigour.

3. Theoretical reminder

3.1 Griffith's analysis

Consider a crack of length a that extends to the surface of a specimen under tensile loading. Since no loads can be transmitted across the crack faces, the stress field in the vicinity of the crack faces vanishes. Part of the elastic energy $(\sigma^2/2E) \cdot V$ stored in the specimen of volume V will thus be released due to the presence of the crack. In order to estimate this energy, Griffith made the assumption that stresses vanish in a (half-)circular zone of radius a around the crack, Fig. 1 (in the case where the crack is located in the centre of the specimen, the stress vanishes in a cylinder of radius a around the crack of length $2a$).

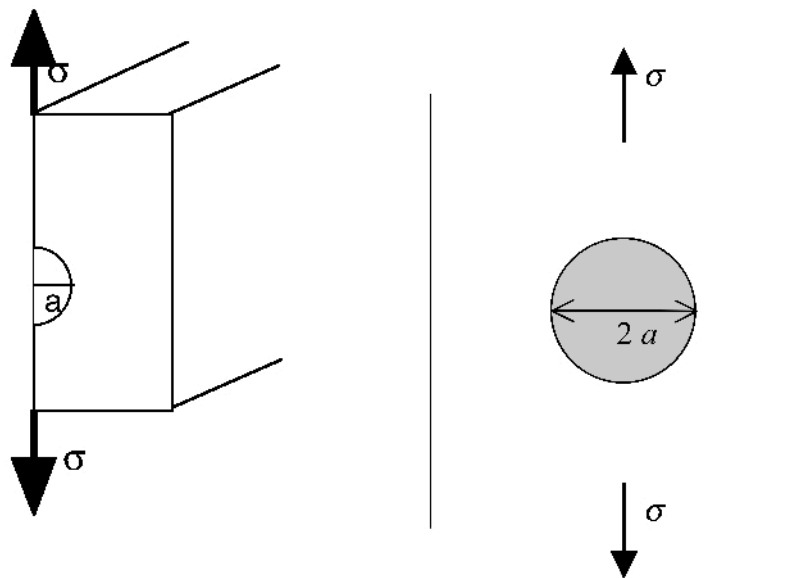


Figure 1. The stored elastic is released in (half-)cylindrical zone of radius a .

The energy released around the crack (considering a plate of unit thickness) thus equals

$$U_e = -\pi a^2 \frac{\sigma^2}{2E}, \quad (1)$$

where E denominates the Young's modulus. Now, the growth of a crack necessitates the creation of surfaces, which consumes energy. Crack propagation is thus hampered by the creation of surfaces. The energy necessary for creating a crack of length a equals

$$U_s = 2a\gamma, \quad (2)$$

where γ is the surface energy of the material in the case where there is no plastic dissipation (otherwise, a correction term is added in order to account for plastic deformation; this case will not be treated here). Summing Eqs. (1) and (2), we obtain the variation of energy that results from crack growth, U_f :

$$U_f = U_e + U_s . \quad (3)$$

The two energy contributions of crack initiation-propagation can be depicted as follows:

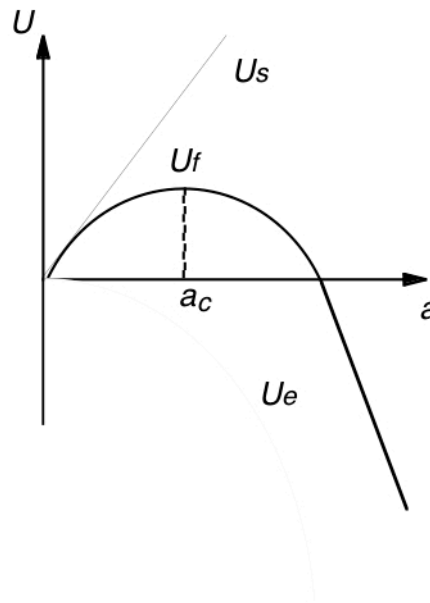


Figure 2. Variation of the crack energy as a function of crack length.

As seen in Fig. 2, the cracking energy passes by a maximum for the crack length a_c . For $a \geq a_c$, crack propagation goes in hand with a decrease of energy of the system. The crack is then unstable and induces immediate fracture of the specimen. We conclude that a crack of length a remains stable as long as $a < a_c$. From the moment where the crack attains his critical value, it is instable and propagates spontaneously under the effect of the applied stress σ . The value of a_c can easily be determined from

$$\left(\frac{\partial U_f}{\partial a} \right)_{a=a_c} = 0 . \quad (4)$$

For a given stress σ , the critical crack length where the crack propagates thus equals

$$a_c = \frac{2\gamma \cdot E}{\sigma^2 \pi} . \quad (5)$$

Alternatively, for a given crack length a , spontaneous crack propagation occurs for a critical stress σ_c :

$$\sigma_c = \sqrt{\frac{2\gamma \cdot E}{\pi a}} . \quad (6)$$

By introducing the concept of the **stress intensity factor** K_I , defined as

$$K_I = \sigma \sqrt{\pi a} , \quad (7)$$

the above said can also be expressed stating that spontaneous crack propagation occurs when this factor attains a limiting value, defined as the material's **critical stress intensity factor** K_{Ic} :

$$K_I \leq K_{Ic} = \sigma_c \sqrt{\pi a} . \quad (8)$$

Since $K_{Ic} = \sqrt{2\gamma \cdot E}$, it follows that this factor is an intrinsic material property and that crack propagation is made more difficult if the material stiffness E and the surface energy γ (and its ductility if plastic dissipation is taken account of as well) are elevated.

As we know when we consider dislocations, the presence of cracks in a metal cannot be avoided. From K_{Ic} we can determine the admissible size of cracks in a structure, depending on testing conditions, applied stress, geometry, etc.

3.2 Stress fields ahead of a crack tip

The assumption that stresses are zero in a region of radius a around the crack is a simplification. A more elaborate analysis of the stress fields ahead of a crack tip (Fig. 3) yields Sneddon's equations for the three principal stresses acting on a volume element:

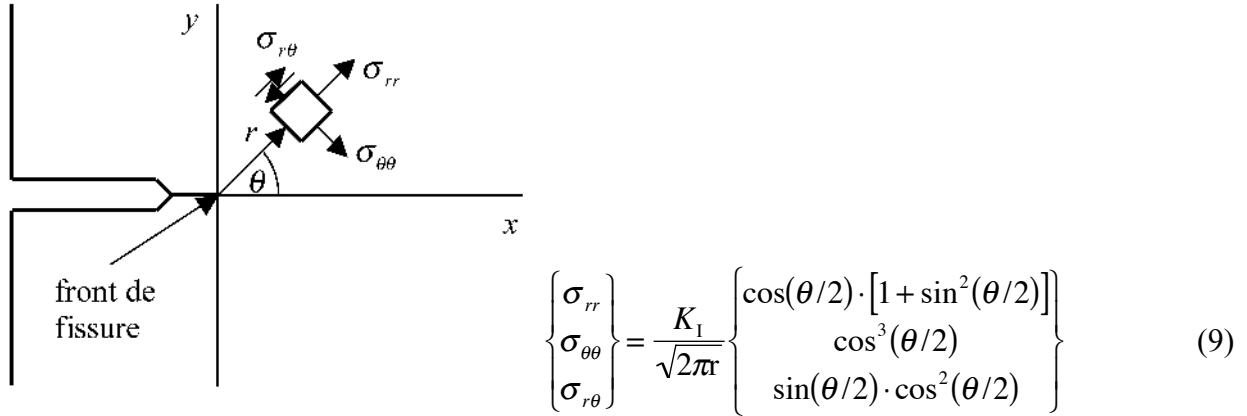


Figure 3. Stress field in a volume element situated at a distance r and an angle θ ahead of the crack tip.

Generally, Sneddon's equations are composed of three factors:

$$\sigma_{ij} = K_I \cdot (2\pi r)^{-1/2} \cdot f_i(\theta) . \quad (10)$$

The first term expresses the stress intensity, whereas the two others represent the radial and angular distribution.

These equations apply for an infinite medium, i.e. for a sample that is infinitely large. In actual testing conditions, samples are of finite size. This is accounted for by introducing a correction factor that depends on specimen geometry, such that the stress intensity factor becomes

$$K_I = \sigma \sqrt{\pi a} \cdot f\left(\frac{a}{W}\right), \quad (11)$$

where f is the correction factor and W the width of the specimen in the direction of crack propagation (see Fig. 4 below).

4. Principle of the test

Several testing geometries exist for assessing the fracture toughness. Here, we employ three-point bend bars. Samples are provided with a notch and a precrack, which is introduced by fatigue. By the aid of a data acquisition programme, the load is recorded as a function of the crack mouth opening displacement. The load P_q that corresponds to a crack extension by 2% of its length has

to be determined. It is found from the intersection of the load curve with a secant from the origin, with a slope that equals 95% of the initial (linear) slope.

K_{Ic} is computed from this load by the aid of equations that are based on the elastic analysis of notched bend bars. For the considered sample geometry, K_{Ic} is computed from the general formula

$$K_{Ic} = \frac{P_q \cdot L}{B \cdot W^{3/2}} \cdot f\left(\frac{a}{W}\right) \quad (12)$$

where B is the specimen thickness, L the length between supports for the 3pt bending test, W the height (width) of the specimen and $f(a/W)$ the correction factor for this geometry, given as

$$f(a/W) = \frac{3 \cdot (a/W)^{1/2} \cdot \left[1.99 - (a/W) \cdot (1 - a/W) \cdot (2.15 - 3.93 \cdot (a/W) + 2.7 \cdot (a/W)^2)\right]}{2 \cdot (1 + 2 \cdot (a/W)) \cdot (1 - a/W)^{3/2}} \quad (13)$$

The relation (12) is based on the assumption that the crack advances in plane strain conditions; in other words, the sample has to be sufficiently thick that plane strain conditions prevail. The criterion for specimen thickness is given as

$$a, B > \frac{2.5 K_{Ic}^2}{\sigma_{ys}^2} \quad (14)$$

where σ_{ys} is the yield strength. If either the thickness B or the crack length a does not satisfy this criterion, the test is not considered valid.

5. Approach via the J -integral

The method for determining the fracture toughness K_{Ic} is based on Griffith's analysis and applies strictly only to linear elastic materials. Within some limits, the method can still be used if crack tip plasticity occurs, but not in the case of more extensive plasticity, as revealed by the violation of the validity requirements of the testing method. A fracture toughness assessment method that extends the limits of validity to materials that exhibit stronger non-linearity is given by the use of the J -integral.

J is the equivalent to G for a non-linear elastic material. As long as loading is proportional (no substantial local unloading due to extensive crack growth), an elastic-plastic material behaves like a non-linear elastic material, and within this limitation the J -integral can then be used to characterize the fracture toughness of elastic-plastic materials. As compared to K_{Ic} assessment,

smaller specimens can be used, which is advantageous notably if specimens of larger dimensions cannot be made from the material available.

The critical value of the J -integral is defined as the value of J where crack initiation occurs. In steels, crack initiation is preceded by crack tip blunting, which typically advances the crack tip by 0.2 mm. Therefore, a crack advance of 0.2 mm is taken as the critical value, and J_{Ic} is then also called $J_{0.2}$ (unless brittle failure occurs before, which also defines critical crack growth). Crack growth is best determined from load–unload cycles. The elastic slope changes with varying specimen compliance, which itself increases with crack advance.

Experimentally, the value of the J -integral is determined from a load vs. CMOD (crack mouth opening displacement) diagram as follows. In standard ASTM E1820, J_{Ic} is determined from

$$J_{Ic} = J_{el} + J_{pl} \quad (15)$$

where J_{el} is the elastic (i.e., linear) component and J_{pl} the plastic (i.e., non-linear) component. J_{el} is determined from K_{Ic} as

$$J_{el} = \frac{K_{Ic}^2(1-\nu^2)}{E} \quad (16)$$

The plastic component J_{pl} is determined from the area under the load vs. CMOD curve, Fig. 4:

$$J_{pl} = \frac{\eta \cdot A_{pl}}{B \cdot (W - a)}, \quad (17)$$

where the correction factor $\eta = 3.785 - 3.101(a/W) + 2.018(a/W)^2$. (18)

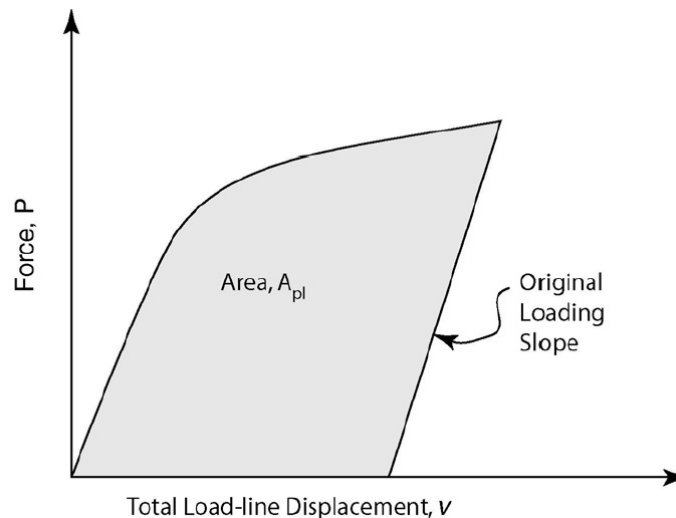


Figure 4. Plastic energy dissipated during a test (ASTM E1820).

In order to compare J_{Ic} fracture toughness values with K_{Ic} values, the former can be expressed as

$$K_{J_{Ic}} = \sqrt{\frac{J_{Ic} E}{(1-\nu^2)}} \quad (19)$$

6. Specimens

The geometry of the setup and dimensions of the 3pt bending-type sample are given in Fig. 4.

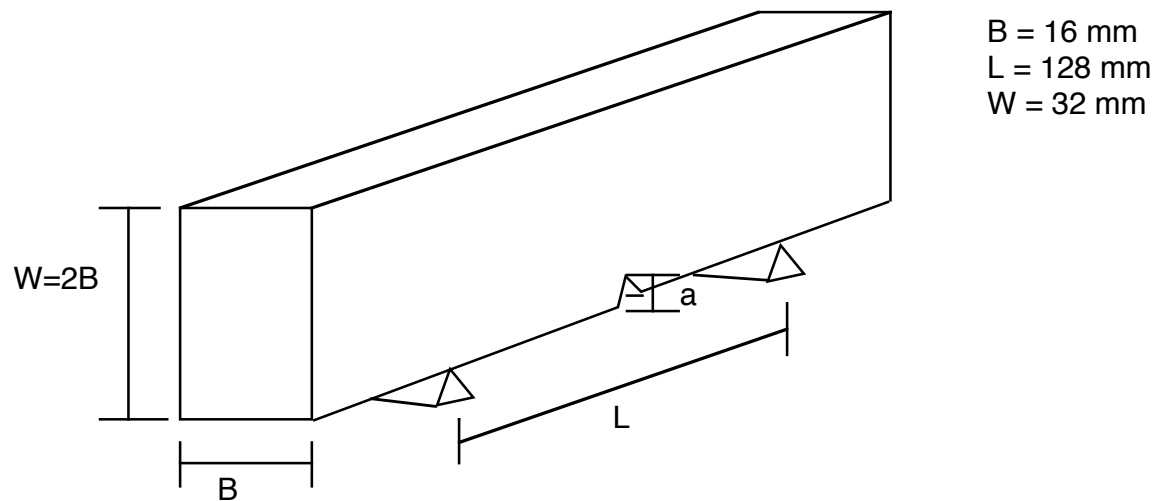


Figure 5. Sketch of the setup and sample dimensions.

Specimens that have undergone the following heat treatments will be tested:

- **N: Normalized** (steel C45E as delivered);
- **T: Water quenched** (*trempe*): water quenched after austenitizing at 850 °C for 1 hr;
- **R: Tempered** (*revenu*): same as **T**, then annealed at 450 °C for 1 hr.

The final stage of sample preparation is fatigue precracking, in order to provide the smallest crack tip radius possible. Precracking is carried out on an "Amsler Vibrophor" machine.

7. Experimental device

Electro-mechanical universal testing machine Schenck equipped with a load cell of 100 kN and controlled with MTS software; HBM Extensometer (model DD1, serial number 98806).

8. Report

The report has to contain the following:

- (i) short theoretical reminder;
- (ii) microstructure of the specimens;
- (iii) description of the experimental procedure;
- (iv) check of the validity of the tests according to the relevant standards;
- (v) computation of K_{Ic} and/or J_{Ic} , and comparison of values with what one can expect from point (ii).

8. Bibliography

- A. Mortensen, *Cours de Déformation et Rupture*, Tome 2, Chapitre VI.
- D. Broek, *Elementary Engineering Fracture Mechanics*, 4th revised edition, Martinus Nijhoff Publisher, Dordrecht (1986).
- N.E. Dowling, *Mechanical Behaviour of Materials*, Prentice-Hall International Editions, New Jersey (1993).
- G.E. Dieter, *Mechanical Metallurgy*, McGraw-Hill Book Company, London (1988).
- J.E. Gordon, *The New Science of Strong Materials (or why you don't fall through the floor)*, Penguin Books, London (1991).
- T.L. Anderson, *Fracture Mechanics: Fundamentals and Applications*, 2nd edition, CRC Press (1995).

Determination of K_{Ic} - Appendix

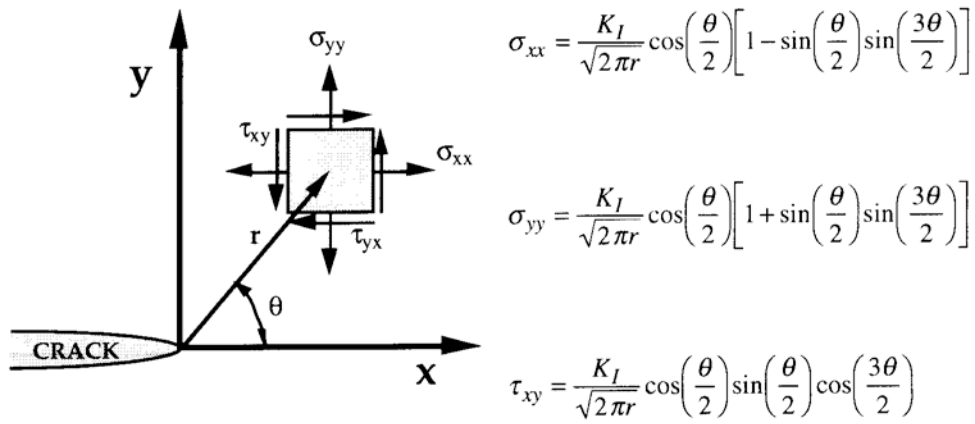
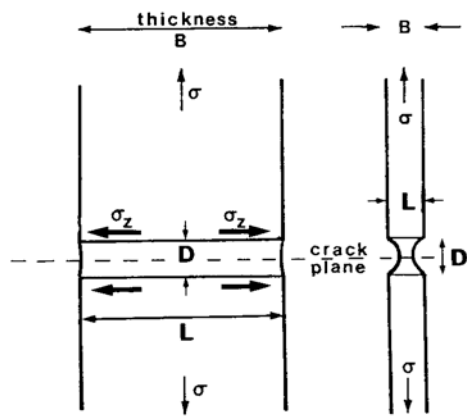
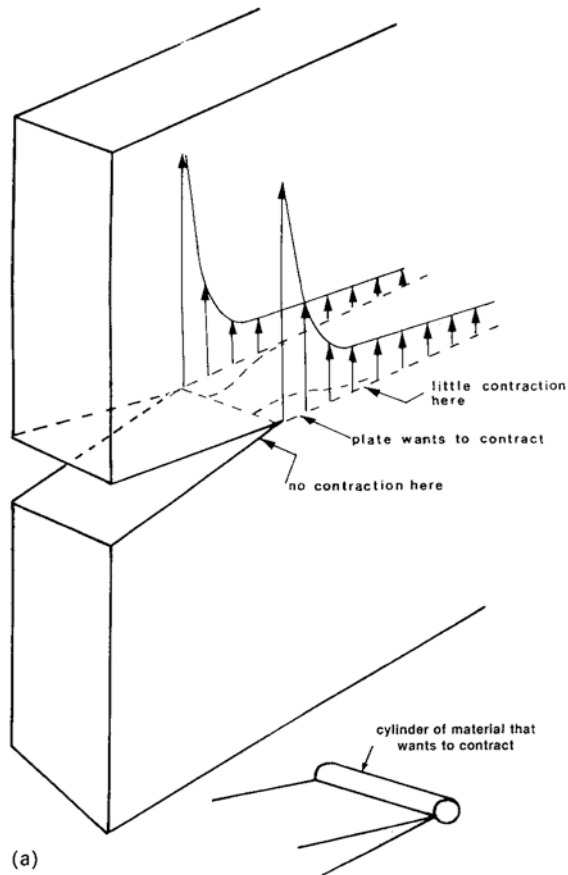


FIGURE 1.9 Stresses near the tip of a crack in an elastic material.



Low stress thick plate,
thin cylinder no contraction
plane strain

Low stress thin plate,
free contraction
plane stress

(b)

Figure 3.7.

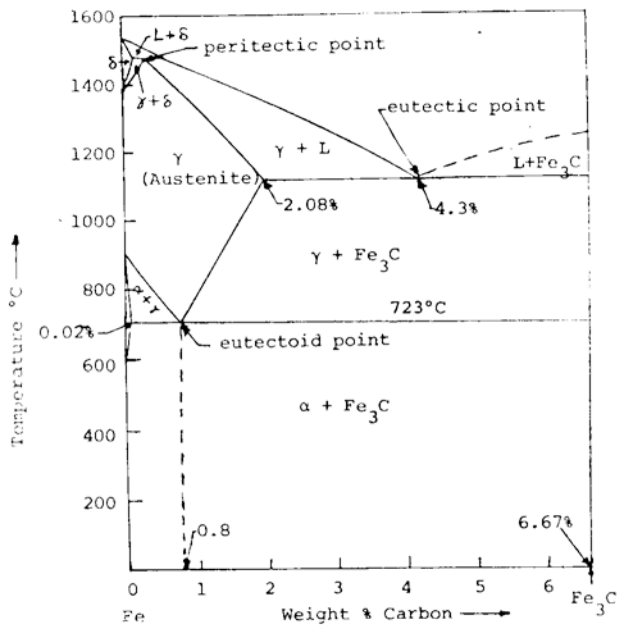


Figure 1-2 The Fe-Fe₃C metastable system. In this binary system, there are three important invariant reactions: peritectic at 1495°C, eutectic at 1148°C, and eutectoid at 723°C.

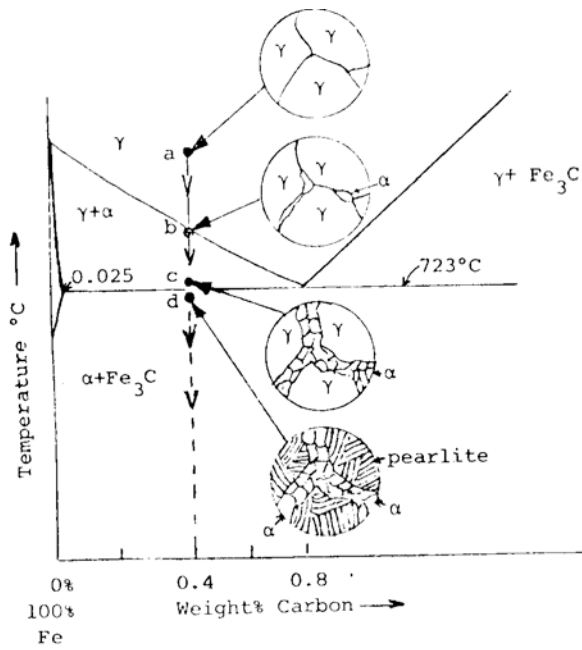


Figure 1-7 Transformation of a 0.4% carbon hypo-eutectoid plain-carbon steel with slow cooling.

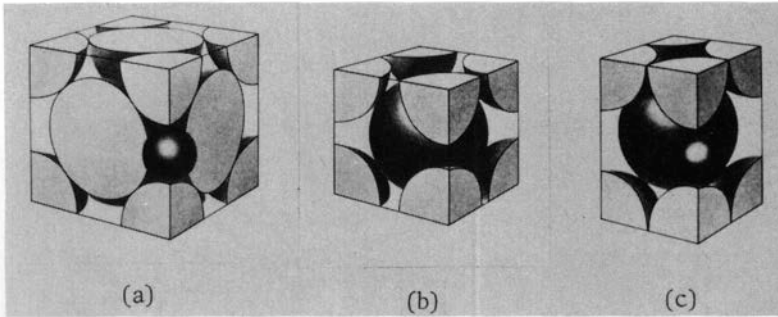


Figure 1-27 Interstitial positions of carbon atoms in FCC, BCC, and BCT iron-crystal structure unit cells. (After E. R. Parker and V. F. Zackay, "Strong and Ductile Steels," *Scientific American*, November, 1968, p. 36. Used by permission.)

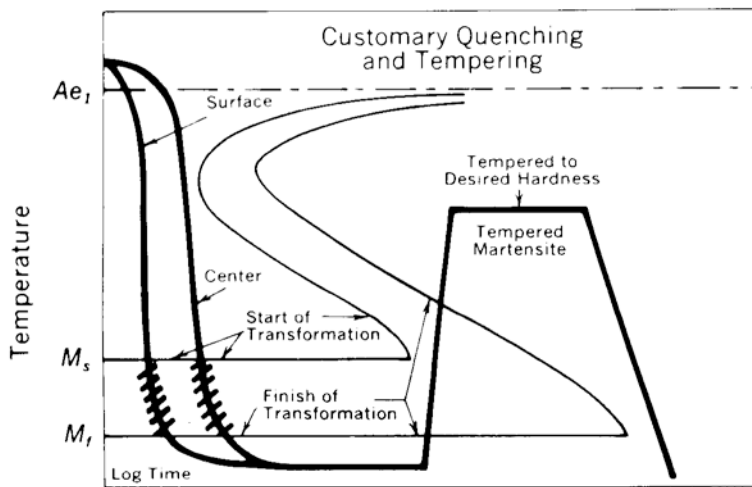


Figure 2-22 Schematic diagram to illustrate the customary quenching and tempering process for a plain-carbon steel. (From "Suiting the Heat Treatment to the Job," *United States Steel Co.*, 1968, p. 34.)

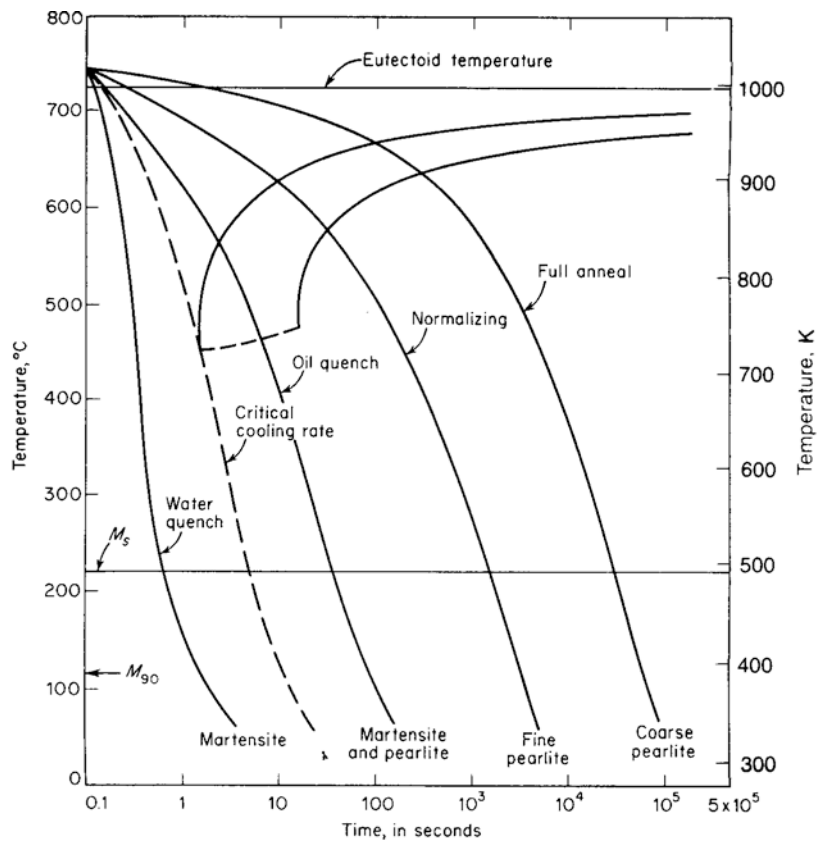


Fig. 19.2 The variation of microstructure as a function of cooling rate for an eutectoid steel.



Figure 2-24 Precipitation of Fe_3C in Fe-0.39% C martensite tempered 1 h at 300°C. (Electron micrograph.) [After G. R. Speich and W. C. Leslie, *Met. Trans.* 3(1972):1043.]